Quantitative interpretation of the transition voltages in gold-poly(phenylene) thiol-gold molecular junctions

Kunlin Wu[1], Meilin Bai[1], Stefano Sanvito[2], Shimin Hou[1, *]

1 Key Laboratory for the Physics and Chemistry of Nanodevices, Department of Electronics, Peking University, Beijing 100871, China

2 School of Physics, AMBER and CRANN Institute, Trinity College, Dublin 2, Ireland

Abstract

The transition voltage of three different asymmetric Au/poly(phenylene) thiol/Au molecular junctions in which the central molecule is either benzene thiol, biphenyl thiol or terphenyl thiol is investigated by first-principles quantum transport simulations. For all the junctions the calculated transition voltage at positive polarity is in quantitative agreement with the experimental values and shows weak dependence on alterations of the Au-phenyl contact. When compared to the strong coupling at the Au-S contact, which dominates the alignment of various molecular orbitals with respect to the electrode Fermi level, the coupling at the Au-phenyl contact produces only a weak perturbation. Therefore, variations of the Au-phenyl contact can only have a minor influence on the transition voltage. These findings not only provide an explanation to the uniformity in the transition voltages found for π-conjugated molecules measured with different experimental methods, but also demonstrate the advantage of transition voltage spectroscopy as a tool for determining the positions of molecular levels in molecular devices.

* The corresponding author. E-mail: smhou@pku.edu.cn

1. Introduction

Understanding electron transport at the single molecule level is critically important in order to further progress the field of molecular electronics [1,2]. The current-voltage, *I-V*, characteristics of a molecular device depends significantly on the alignment of various molecular levels with respect to the Fermi level, E_F, of the electrodes. Transition voltage spectroscopy (TVS), which was recently introduced by Beebe *et al.* [3,4], is a non-destructive electrical-based technique for characterizing molecular energy levels in molecular devices. Due to its simplicity and sensitivity, TVS is becoming an increasingly popular spectroscopic tool for molecular devices [5-18], and recently it has been even extended to characterize Au/vacuum/Au junctions [19]. In constructing molecular junctions, π-conjugated molecules and alkyl chains are often chosen as the central molecule. However, TVS experimental results for these two kinds of molecules are quite different. In contrast to alkyl chains connected to gold electrodes through the Au-S bonds whose transition voltages are distributed over a wide range going from 0.7 V to 1.9 V [4,8,10,13,16,17], the measured transition voltages for π-conjugated molecules are surprisingly much more uniform [3,4,9,14,17]. For example, the transition voltages of Au/terphenyl thiol/Au junctions are respectively measured to be 0.67±0.14 V [3,4] and 0.69±0.3 V [9], and that of the Au/terphenyl dithiol/Au junctions is determined to be about 0.7 V [14].

When interpreting TVS measurements for molecular devices, it has been accepted that the coherent Landauer transport formalism is more appropriate than considering models for tunneling over an energy barrier [20]. Furthermore, it is established that the transition voltage is related to the applied bias voltage, which promotes a significant spectral weight of the transmission function into the bias window [21]. However, most theoretical studies focus on the general properties of the transition voltage using generic phenomenological models [20-28] while very few studies have considered the detailed atomic structures of the device [21,29,30]. More importantly, there are no atomistic calculations reproducing the measured values of the transition voltage of real junctions. For example, in references [21] and [29] the transition voltages of Au/benzene thiol/Au junctions are calculated to be 0.32 V and 1.69 V, far from the experimental value of 0.95±0.11 V [3,4]. Therefore, in order to gain a deeper insight into TVS of molecular devices, it is highly desirable to perform first-principles calculations taking explicitly into account the exact nature of the molecule and the electrode-molecule interfaces so that to obtain a quantitative interpretation of TVS measurements.

In order to address these questions, we investigate theoretically the electronic transport properties of gold-poly(phenylene) thiol-gold molecular junctions, which include three molecules:

benzene thiol, biphenyl thiol and terphenyl thiol. This is realized by employing the non-equilibrium Green's function formalism combined with density functional theory (i.e., the NEGF+DFT approach) [31-40]. Our calculations show that the asymmetric couplings at the Au-S and Au-phenyl contacts play an important role in determining the transition voltage. The strong electronic coupling at the Au-S contact dominates the alignment of various molecular levels relative to the electrode Fermi level. In contrast, the coupling at the Au-phenyl contact is much weaker and cannot affect the alignment significantly. Therefore, the calculated transition voltages show a weak dependence on the variations of the Au-phenyl contacts including the Au-H distance and the electrode shape. When the sulfur atom binds between the bridge and hollow sites of the Au(111) surface, the calculated transition voltages for these three kinds of gold-poly(phenylene) thiol-gold molecular junctions are in quantitative agreement with the experiments [3,4,9].

2. Calculation method

In this work we use the SIESTA code [41] to study the atomic structure of Au/poly(phenylene) thiol/Au molecular junctions and the quantum transport code SMEAGOL [38-40] to study their electronic transport properties. SIESTA is an efficient DFT package, which adopts a finite-range numerical orbital basis set to expand the wave functions of the valence electrons and makes use of improved Troullier–Martins pseudopotentials for the atomic cores [41,42]. While a double-zeta plus polarization (DZP) basis set is used for H, C and S, two different types of basis functions are used for Au, respectively in the bulk and at the surface. In more detail, a double-zeta basis set augmented with polarization and diffuse functions (DZP+diffuse) is used for the surface Au atoms, while a single-zeta plus polarization (SZP) basis is used for the bulk. This allows us to keep a balance between the efficiency and the required accuracy of the simulations [43,44]. The Perdew–Burke–Ernzerhof (PBE) generalized gradient approximation (GGA) to the exchange and correlation functional is used in all our calculations to account for the electron–electron interaction [45]. Geometry optimization is performed by standard conjugate gradient relaxation until the atomic forces are smaller than 0.03 eV $Å^{-1}$.

SMEAGOL is a practical implementation of the NEGF+DFT approach, which employs SIESTA as the DFT platform [38-40]. We use an equivalent cutoff of 200.0 Ryd for the real space grid. The charge density is integrated over 36 energy points along the semi-circle, 36 along the line in the complex plane, 240 along the real axis, while 36 poles are used for the Fermi function (the electronic temperature is 25 meV). We always consider periodic boundary conditions in the plane transverse to the transport. The unit cell of the extended molecule, for which the self-consistent calculation is performed, comprises the poly(phenylene) thiol molecule

and ten Au(111) atomic layers with a (3×3) in plane supercell. The *I–V* curve of the junction is calculated as

$$I = \frac{2e}{h}\int_{-\infty}^{+\infty} T(V,E)[f(E-\mu_L) - f(E-\mu_R)]dE, \quad (1)$$

where *T (V, E)* is the bias *V* dependent transmission coefficient of the junction, *f (E)* is the Fermi function, $\mu_{L/R} = E_F \pm eV/2$ is the local Fermi level of the left/right gold electrode. The transition voltage is obtained from the minimum appearing in the Fowler-Nordheim (F-N) plot of the *I-V* data, i.e. a plot of $\ln(I/V^2)$ against 1/V. Then, the total transmission coefficient *T(V, E)* of the junction is evaluated as

$$T(V,E) = \frac{1}{\Omega_{2DBZ}}\int_{2DBZ} T(\vec{k};V,E)d\vec{k}, \quad (2)$$

where Ω_{2DBZ} is the area of the two-dimensional Brillouin zone (2DBZ) in the transverse directions. The *k*-dependent transmission coefficient $T(\vec{k};V,E)$ is obtained as

$$T(\vec{k};V,E) = Tr[\Gamma_L G_M^R \Gamma_R G_M^{R+}], \quad (3)$$

where G_M^R is the retarded Green's function matrix of the extended molecule and $\Gamma_{L(R)}$ is the broadening function matrix describing the interaction of the extended molecule with the left (right) electrode. Here, we calculate the transmission coefficient by sampling 4×4 k-points in the transverse 2DBZ.

3. Results and discussion

We start our studies from the investigation on the electronic transport properties of the Au/biphenyl thiol/Au molecular junction. As shown in Fig. 1(a), the biphenyl thiol molecule is assumed to be sandwiched between two gold electrodes with an atomically flat Au(111) surface. After optimization, the sulfur atom is found to be located between the bridge and hollow sites with an average Au-S bond length of 2.57Å and the shortest Au-H distance at the opposite side is calculated to be 3.08 Å. The equilibrium transmission spectrum of this Au/biphenyl thiol/Au junction is given in Fig. 1(b). Since the direct coupling between the phenyl ring and the gold electrode is rather weak, $T(V=0, E_F)$ is only 5.6×10^{-4}. In more details, around the Fermi level three broad transmission peaks appear respectively at -1.66 eV, -0.96 eV and 2.51 eV. Eigenchannel analysis [46,47] reveals that these three transmission peaks originate respectively from the biphenyl thiol HOMO-1, HOMO and LUMO molecule orbitals (Fig. S1 in the Supplementary Material) [48]. Here, HOMO and LUMO are acronyms for the highest occupied molecular orbital and the lowest unoccupied molecule orbital. All these three frontier molecular orbitals are

π-type delocalized along the entire molecule including the S atom of the binding group, thus they have a strong interaction with the gold electrodes.

When compared to the LUMO-related transmission peak, the HOMO-dominated one is closer to the Fermi level. Its peak value approaches 0.01, i.e. it is much large than the value of T at the Fermi level, thus one can expect that the current through the junction will increase quickly after the tail of the HOMO enters the bias window. This is indeed the case when a positive bias voltage is applied to the gold electrode connected to the biphenyl thiol molecule through the Au-phenyl interface (Fig. 1c). As one can clearly see, the current increases linearly at low bias but then increases rapidly after the bias exceeds 0.5 V. Correspondingly, a well-defined minimum appears in the F-N plot and the transition voltage is determined to be 0.7 V. This value is in good agreement with the experimentally determined one of 0.81±0.11 V [3,4]. The bias-dependent transmission spectra confirm this picture (Fig. 1d). By increasing the bias, the HOMO transmission peaks move almost rigidly to higher energies. As soon as the HOMO-dominated transmission peak enters the bias window, the current through the junction increases non-linearly. As a consequence, at such value of the bias an inflection appears in the F-N plot, demonstrating that the transition voltage of the Au/biphenyl thiol/Au junction at the positive polarity is related to the HOMO of the biphenyl thiol molecule. This is also corroborated by the thermoelectric measurements on the Au/biphenyl thiol/Au junction [49], in which the obtained positive thermopower (Seebeck coefficient) has unambiguously shown that the HOMO of the biphenyl thiol molecule is closer to the Fermi level that the LUMO.

In both conducting-probe atomic force microscopy and cross-wire tunneling junctions [3,4], the exact nature of the Au-phenyl interface is unknown. Here, in order to understand how strongly the transition voltage is sensitive to the details of the junction geometry, we first investigate its dependence on the Au-phenyl distance. To this goal Fig. 2 shows that, when the Au-H distance is increased from 2.41 Å to 4.98 Å, the transmission coefficient at E_F reduces from 3.6×10^{-3} to 2.5×10^{-6}, a change of more than three orders of magnitude. In contrast, the transition voltage changes very little, only decreasing from 0.8 V to 0.65 V. Such result is easy to understand. In these asymmetric junctions, the biphenyl thiol molecule only interacts strongly with one gold electrode, namely the one presenting the Au-S bond. This determines the broadening of all molecular orbitals and their alignment relative to the electrode Fermi level. The main effect originating from varying the Au-phenyl distance is to define the tunneling barrier width at the Au-phenyl interface, so that increasing the Au-phenyl distance significantly reduces the transmission coefficients but does not change the overall shape of the transmission spectra

(see Fig. S2 in the Supplementary Material). Such feature gives rise to a weak distance-dependence of the transition voltage.

Then we move to investigate the influence of the electrode shape on the transition voltage. As an example we consider bonding the phenyl ring to the Au(111) surface of the gold electrode through one gold adatom (see Fig.3a). Compared with the junction not presenting the gold adatom (Fig.1a), the Au-S bond is intact and the Au-H distance is decreased to 2.70 Å. Since the gold adatom further reduces the coupling between the phenyl ring and the gold electrode, not only the transmission coefficient at the Fermi level is decreased to 7.5×10^{-5}, but also the two transmission peaks contributed by the biphenyl thiol HOMO and LUMO are strongly suppressed (Fig. 3b). In contrast, the transmission peak related to the HOMO-1 is significantly enhanced. Therefore, the electrode shape does somehow affect the junction transmission. However, the transition voltage determined from the corresponding F-N plot is 0.75 V (Fig. 3c), much close to that of the junction shown in Fig. 1a, and does not depend on the specific Au-H distance. In fact, when the Au-H distance is elongated to 3.67 Å, the transition voltage still remains 0.75 V. Even bonding the phenyl ring to the Au(111) surface of the gold electrode through one gold cluster with four atoms arranged in a pyramid configuration gives a transition voltage of 0.7 V (see Fig. S3 in the Supplementary Material). The robustness of the transition voltage in the Au/biphenyl thiol/Au junctions with respect to the variations of the Au-phenyl interface still originates from the asymmetric coupling at its two contacts. Variations of the Au/phenyl interface (distance, electrode shape, etc) significantly affect the tunneling barrier and thus result in large changes of the junction transmission and current. However, the Au/phenyl electronic coupling is only a weak perturbation of the total coupling of the molecule to the electrode, which is dominated by the thiol/Au bond. Thus the Au/phenyl interface has only a minor influence on the alignment of the molecular orbitals (Fig. 3d). This feature not only explains the experimental fact that π-conjugated thiol molecular junctions fabricated with different methods can deliver very similar transition voltages, but also demonstrates that TVS is indeed a perfect spectroscopic tool for determining the positions of molecular levels in electronic devices.

It should be noted that, at variance with the Au/phenyl interface, alterations of the Au-S bonds have a significant influence on the transition voltage of the junction. For example, when the sulfur atom binds at the adatom site (see Fig. S4 in the Supplementary Material), the HOMO-dominated transmission peak is shifted up to -0.28 eV and its tail also extends beyond the Fermi level, leading to a large transmission at E_F. As a result, the current increases very slowly, and no minimum appears in the F-N plot up to voltages as large as 1.0 V.

Now we extend our studies to the benzene thiol and terphenyl thiol molecules. Taking the same geometric structure as that of the Au/biphenyl thiol/Au junction (Fig. 1a), both the benzene thiol and terphenyl thiol molecules are sandwiched between two gold electrodes with an atomically flat Au(111) surface, and the sulfur atom is bonded between the bridge and hollow sites (Fig. 4). For a Au-phenyl distance of about 3.4 Å, the transition voltages of the Au/benzene thiol/gold junction and the Au/terphenyl thiol/Au junction are respectively calculated to be 0.9 V and 0.6 V, which are both in quantitative agreement with the measured values (0.95±0.11 V and 0.67±0.14 V) [3,4]. We have also checked the dependence of the transition voltages of these two junctions on the geometrical structures of the Au/phenyl interface, and found that neither the Au-phenyl distance nor the electrode shape affects the transition voltages significantly (see figures S5 and S6 in the Supplementary Material). Only one exception occurs for the Au/benzene thiol/Au junction when the electrode at the Au-phenyl interface is decorated with one gold cluster in the pyramid configuration, in which the FN plot around 1.0 V is very flat and no minimum can be observed. This difference is intimately related to the electronic structure of the benzene thiol molecule. Compared with the junctions composed of the other two aromatic thiol molecules, the HOMO-dominated transmission peak of the Au/benzene thiol/Au junction is far from other transmission peaks thus its overall shape is easily affected by the junction structure and the transition voltage is relatively prone to the change of the electrode shape at the Au-phenyl interface.

It should be noted that a much lower value (0.32 V) for the transition voltage of the Au/benzene thiol/Au junction is reported in reference 21, though a junction structure similar to Fig. 4a is adopted. The authors ascribe this big discrepancy to the local density approximation (LDA) for the DFT exchange-correlation functional. In order to check whether the LDA and GGA functionals will significantly affect the calculation on the transition voltage, we recalculate the I-V characteristics of the Au/benzene thiol/Au junction shown in Fig. 4a using the Pewdew-Zunger LDA functional [50], and the transition voltage is determined to be 0.83 V, very close to the value obtained with the PBE GGA functional (see Fig. S7 in the Supplementary Material). Therefore, the underestimation of the transition voltage of the Au/benzene thiol/Au junction in reference 21 is not caused by the LDA functional but might be due to the constructed junction model (not enough electrode atoms included in the extended molecule) and other calculation parameters (for example, the too small single-zeta plus polarization basis set).

Comparing the equilibrium transmission spectra of these three different Au/poly(phenylene)-thiol/Au junctions (Fig.1b, Fig. 4a and Fig. 4c), we can see that improvements in the conjugation make the HOMO-dominated transmission peak moving toward the Fermi level. Thus the

transition voltage decreases from 0.9 V for benzene to 0.7 V for biphenyl to 0.6 V for terphenyl. The LUMO-dominated transmission peak also moves toward E_F, because the conjugation has the effect of reducing the HOMO-LUMO gap. Thus, one can expect that the transition voltage of the Au/terphenyl thiol/Au junction should also be smaller than those of the other two junctions when the bias polarity is reversed. Experimental measurements support this conjecture. When the applied bias is swept from -1.0 V to +1.0 V, a transition voltage at negative bias is observed only for terphenyl thiol [3] and it is measured to be between -0.82 V and -0.92 V depending on the fabrication method. For the other two molecules no inflection is found in the F-N plots. Thus, we have investigated the transition voltage of the Au/terphenyl thiol/Au junction when a negative bias is applied. The calculated *I-V* curve and the corresponding F-N plot are presented in Fig. 5 (here the Au-phenyl distance is set to 2.67 Å). When compared to the positive polarity, the current under the negative bias increases more slowly and the transition voltage is determined to be -1.5 V, more than 50% higher than the measured value [3]. Furthermore, the distance dependence of the transition voltage at the negative polarity is much more pronounced. When the Au-phenyl distance is increased from 2.67 Å to 3.38 Å and finally to 4.29 Å, the transition voltage changes from -1.5 V to -1.7 V to -1.8 V. It is difficult to rationalize such large discrepancy, exceeding a factor two, between theory and experiments. The anomalous situation arises because the measured transition voltage is smaller than the calculated one. Following the argument made so far, this means that the experimental LUMO is significantly closer to E_F than the one calculated at the GGA level. Since the HOMO seems to be at the right place this means that the measured transport HOMO-LUMO gap is significantly smaller than the GGA one. Although HOMO-LUMO gap renormalization at an organic/inorganic interface is expected because of dynamical charge transfer [51-53], it is difficult to believe that this is the sole cause of such low LUMO state. At present we do not have a rationale explanation for the exact origin of such discrepancy between theory and experiments and further investigation, both experimental and theoretical, will be needed to clarify the issue.

4. Conclusion

We have investigated the transition voltage of three kinds of Au/poly(phenylene) thiol/Au molecular junctions using the NEGF+DFT approach, and found that asymmetric couplings at the two contacts play a critical role in their electronic transport properties. Due to the strong Au-S covalent bonds, the coupling at the thiol end dominates the alignment of various molecular levels with respect to the electrode Fermi energy. In contrast, the coupling at the Au-phenyl contact produces only a weak perturbation to the alignment, though it has significant influences on the

junction transmission and thus on the current through the junction. Therefore, the transition voltage at positive and negative polarities are respectively related to the HOMO and LUMO of the corresponding poly(phenylene) thiol molecule. For positive polarity, our calculated transition voltages are all in quantitative agreement with the measured values, and also show a weak dependence on the variations of the Au-phenyl contact. This not only explains the uniformity of the transition voltages measured with different experimental methods, but also demonstrates the advantage of TVS as a spectroscopic tool in determining the positions of molecular levels in a junction. However, the calculated transition voltages at the negative polarity are much larger than the measured values and more effort is needed to solve such a puzzle.

Acknowledgement

This project was supported by the National Natural Science Foundation of China (No. 61071012) and the MOST of China (Nos. 2011CB933001 and 2013CB933404). SS thanks additional funding support from Science Foundation of Ireland (grant no. 07/IN/I945), by KAUST (FIC/2010/08) and by CRANN.

Reference

[1] N.J. Tao, Nat. Nanotechnol. 1, 173 (2006).

[2] H. Song, M.A. Reed, T. Lee, Adv. Mater., 23, 1583(2011)

[3] J.M. Beebe, B. Kim, J.W. Gadzuk, C.D. Frisbie, J.G. Kushmerick, Phys. Rev. Lett., 97, 026801(2006).

[4] J.M. Beebe, B. Kim, C.D. Frisbie, J.G. Kushmerick, ACS Nano, 2, 827(2008)

[5] K. Liu, X. Wang, F. Wang, ACS Nano, 2, 2315(2008)

[6] AV. Pakoulev, V.Burtman, J. Phys. Chem. C, 113, 21413(2009)

[7] G.Wang, T.-W. Kim, G. Jo, T. Lee, J. Am. Chem. Soc., 131, 5980(2009)

[8] H. Song, Y. Kim, Y.H. Jang, H. Jeong, M.A. Reed, T. Lee, Nature, 1039(2009)

[9] A. Tan, S. Sadat, P. Reddy, Appl. Phys. Lett. 96, 013110 (2010)

[10] G. Noy, A. Ophir, Y. Selzer, Angew. Chem. Int. Ed., 49, 5734(2010)

[11] N. Bennett, G. Xu, L.J. Esdaile, H.L. Anderson, J.E. Macdonald, M. Elliott, Small, 6, 2604(2010)

[12] S.H. Choi, C. Risko, M.C.R. Delgado, B. Kim, J.-L. Brédas, C.D. Frisbie, J. Am. Chem. Soc., 132, 4358(2010)

[13] H. Song, Y. Kim, H. Jeong, M.A. Reed, T. Lee, J. Phys. Chem. C, 114, 20431(2010)

[14] H. Song, Y. Kim, H. Jeong, M.A. Reed, T. Lee, J. Appl. Phys. 109, 102419 (2011)
[15] G.Wang, Y. Kim, S.-I. Na, Y.H. Kahng, J. Ku, S. Park, Y.H. Jang, D.-Y. Kim, T. Lee, J. Phys. Chem. C, 115, 17979(2011)
[16] D. Xiang, Y. Zhang, F. Pyatkov, A. Offenhäusser, D. Mayer, Chem. Commun., 47, 4760(2011)
[17] S. Guo, J. Hihath, I. Díez-Pérez, N. Tao, J. Am. Chem. Soc., 133, 19189(2011)
[18] G. Ricoeur, S. Lenfant, D. Guérin, D. Vuilaume, J. Phys. Chem. C, 116, 20722(2012)
[19] M.L. Trouwborst, C.A. Martin, R.H.M. Smit, C.M. Guédon, T.A. Baart, S.J. van der Molen, J. M. van Ruitenbeek, Nano Lett., 11, 614(2011)
[20] E.H. Huisman, C.M. Guédon, B.J. van Wees, S.J. van der Molen, Nano Lett., 9(2009)3909
[21] M. Araidai, M. Tsukada, Phys. Rev. B, 81, 235114(2010)
[22] I. Bâldea, Chem. Phys., 377, 15(2010)
[23] F. Mirjani, J.M. Thijssen, S.J. van der Molen, Phys. Rev. B, 84, 115402 (2011)
[24] I. Bâldea, Phys. Rev. B, 85, 035442 (2012)
[25] I. Bâldea, H. Köppel, Phys. Lett. A, 376, 1472(2012)
[26] I. Bâldea, Chem. Phys., 400, 65(2012)
[27] I. Bâldea, J. Am. Chem. Soc, 134, 7958(2012)
[28] A. Vilan, D. Cahen, E. Kraisler, ACS Nano, 7, 695(2013)
[29] J. Chen, T. Markussen, K.S. Thygesen, Phys. Rev. B, 82, 121412(R)(2010)
[30] T. Markussen, J. Chen, K.S. Thygesen, Phys. Rev. B, 83, 155407 (2011)
[31] Y. Meir, N.S. Wingreen, Phys. Rev. Lett. 68, 2512 (1992).
[32] P. Hohenberg, W. Kohn, Phys. Rev. 136, B864 (1964).
[33] W. Kohn, L.J. Sham, Phys. Rev. 140, A1133 (1965).
[34] Y. Xue, S. Datta, M.A. Ratner, Chem. Phys. 281, 151 (2002).
[35] M. Brandbyge, J.-L. Mozos, P. Ordejón, J. Taylor, K. Stokbro, Phys. Rev. B 65, 165401 (2002).
[36] J. Zhang, S. Hou, R. Li, Z. Qian, R. Han, Z. Shen, X. Zhao, Z. Xue, Nanotechnology 16, 3057 (2005).
[37] R. Li, J. Zhang, S. Hou, Z. Qian, Z. Shen, X. Zhao, Z. Xue, Chem. Phys. 336, 127(2007)
[38] A.R. Rocha, V.M. Garcia-Suarez, S.W. Bailey, C.J. Lambert, J. Ferrer, S. Sanvito, Nature Mater. 4, 335 (2005).
[39] A.R. Rocha, V.M. García-Suárez, S. Bailey, C. Lambert, J. Ferrer, S. Sanvito, Phys. Rev. B 73, 085414 (2006).

[40] I. Rungger and S. Sanvito, Phys. Rev. B 78, 035407 (2008).

[41] J.M. Soler, E. Artacho, J.D. Gale, A. García, J. Junquera, P. Ordejón and D. Sánchez-Portal, J. Phys.: Condens. Matter 14, 2745 (2002).

[42] N. Troullier, J. Martins, Phys. Rev. B, 43, 1993 (1991).

[43] S. García-Gil, A. García, N. Lorente, P. Ordejón, Phys. Rev. B, 79, 075441(2009)

[44] K. Wu, M. Bai, S. Sanvito, S. Hou, Nanotechnology, 24, 025203(2013)

[45] J. Perdew, K. Burke, M. Ernzerhof, Phys. Rev. Lett. 77, 3865 (1996)

[46] R. Li, S. Hou, J. Zhang, Z. Qian, Z. Shen, X. Zhao, J. Chem. Phys., 125, 194113 (2006)

[47] M. Paulsson, M. Brandbyge, Phys. Rev. B, 76, 115117(2007)

[48] See Supplementary Material Document No._____ for the eigenchannel analysis and the transmission spectra at different gold-phenyl distances of the Au/biphenyl thiol/Au junction with the phenyl ring bonded to the Au(111) surface directly, the geometrical structure and the transport properties of the Au/biphenyl thiol/Au junctions with the phenyl ring bonded to the Au(111) surface through a four-atom gold cluster in a pyramid configuration and with the sulfur atom binding at the adatom site of the Au(111) surface, the geometrical structure and the transport properties of the Au/benzene thiol/Au and Au/terphenyl thiol/Au junctions with the phenyl ring bonded to the Au(111) surface through a gold adatom or a four-atom gold cluster, and the transport properties of the Au/benzene thiol/Au junction calculated using the LDA functional.

[49] A. Tan, J. Balachandran, B.D. Dunietz, S.Y. Jang, V. Gavini, P. Reddy, Appl. Phys. Lett., 101, 243107(2013)

[50] J.P. Perdew, Z. Zunger, Phys. Rev. B, 23, 5048(1981)

[51] J.B. Neaton, M.S. Hybertsen, S.G. Louie, Phys. Rev. Lett., 97, 216405 (2006)

[52] K.S. Thygesen, A. Rubio, Phys. Rev. Lett., 102, 046802 (2009)

[53] M. Strange, C. Rostgaard, H. Häkkinene, K.S. Thygesen, Phys. Rev. B, 83, 115108 (2011)

Figure captions

Figure 1 The optimized atomic structure (a), the equilibrium transmission spectrum (b), the F-N plot (c) and the bias-dependent transmission spectra (d) of the Au/biphenyl thiol/Au junction. The spectra except for V=0 are vertically offset for clarity, and the inset in (c) shows the I-V curve on a linear scale. Here, the biphenyl thiol molecule is sandwiched between two gold electrode with an atomically flat Au(111) surface.

Figure 2 The distance dependence of the transition voltage and the transmission coefficient at the Fermi level of the Au/biphenyl thiol/Au junction.

Figure 3 The optimized atomic structure (a), the equilibrium transmission spectrum (b), the F-N plot (c) of the Au/biphenyl thiol/Au junction, in which the phenyl ring is connected to the Au(111) surface through one gold adatom. (d) Comparison of the local density of states (LDOS) of the biphenyl thiol molecule in the junctions with and without the gold adatom.

Figure 4 The equilibrium transmission spectrum (a) and the F-N plot of the Au/benzene thiol/Au junction, the inset in (a) shows its optimized atomic structure and the insert in (b) is its I-V curve on a linear scale; The same quantities for the Au/terphenyl thiol/Au junction is given in panels (c) and (d).

Figure 5 The I-V curve on a linear scale (a) and the corresponding F-N plot (b) of the Au/terphenyl thiol/Au junction at negative bias voltages

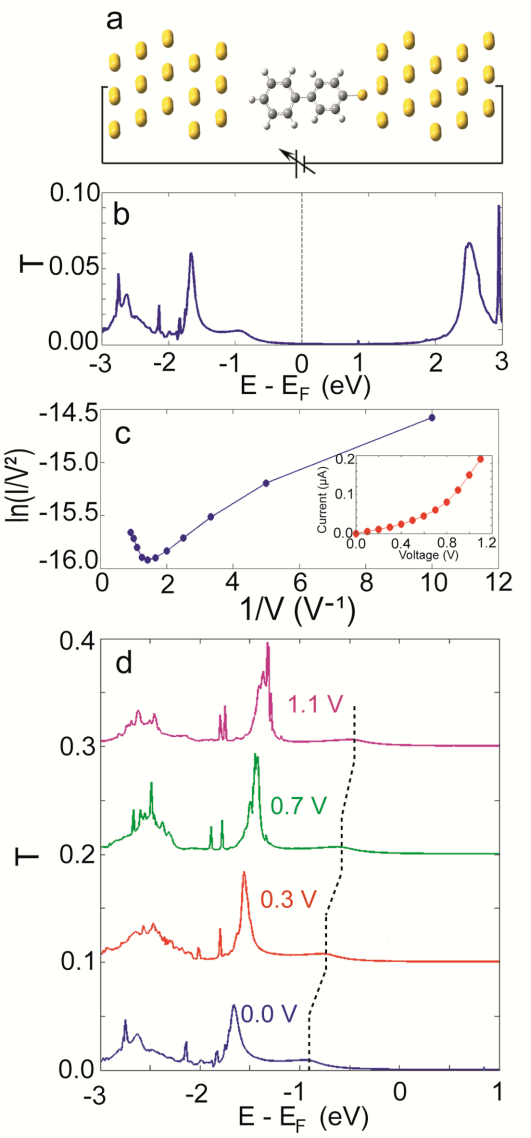
a
b
T
0.10
0.05
0.00
-3
-2
-1
0
1
2
3
E - E_F (eV)
c
ln(I/V²)
-14.5
-15.0
-15.5
-16.0
0
2
4
6
8
10
12
1/V (V⁻¹)
Current (μA)
0.2
0.1
0.0
0.0
0.4
0.8
1.2
Voltage (V)
d
T
0.4
0.3
0.2
0.1
0.0
1.1 V
0.7 V
0.3 V
0.0 V
-3
-2
-1
0
1
E - E_F (eV)

Figure 1

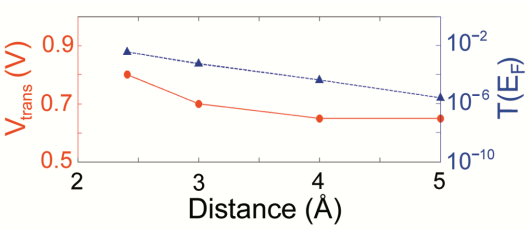

Figure 2

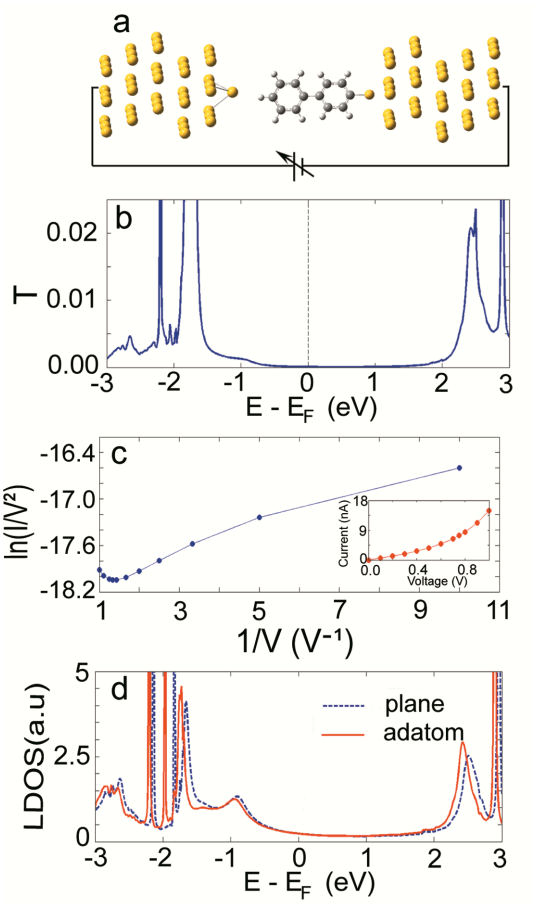
a
b
T
0.02
0.01
0.00
-3
-2
-1
0
1
2
3
E - E_F (eV)
c
ln(I/V²)
-16.4
-17.0
-17.6
-18.2
1
3
5
7
9
11
1/V (V⁻¹)
Current (nA)
18
9
0
0.0
0.4
0.8
Voltage (V)
d
LDOS(a.u)
5
2.5
0
plane
adatom
E - E_F (eV)

Figure 3

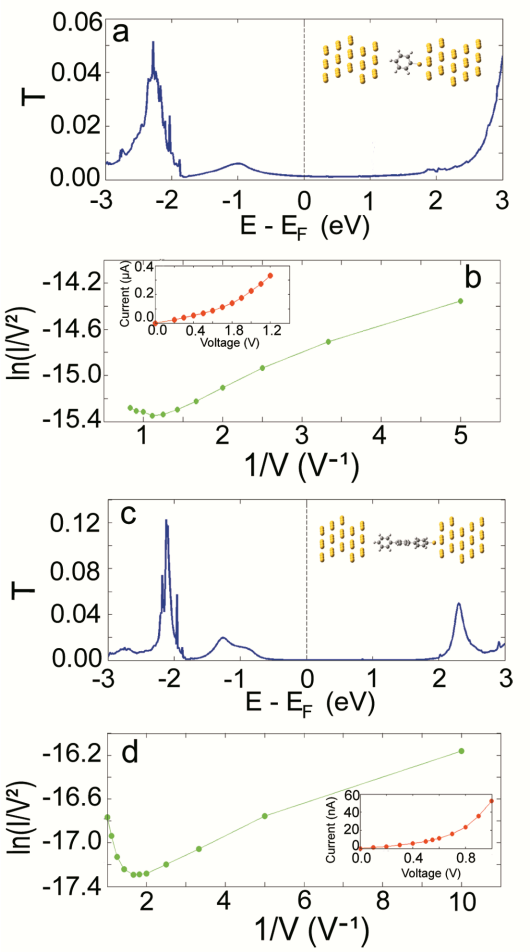
a
T
E - E_F (eV)
b
ln(I/V²)
1/V (V⁻¹)
Current (μA)
Voltage (V)
c
T
E - E_F (eV)
d
ln(I/V²)
1/V (V⁻¹)
Current (nA)
Voltage (V)

Figure 4

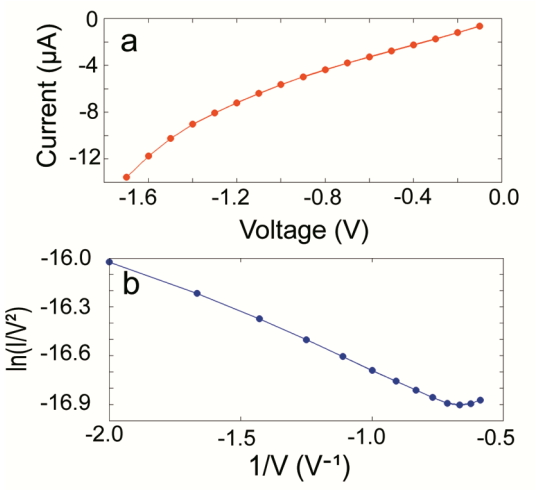
a
Current (μA)
0
-4
-8
-12
-1.6
-1.2
-0.8
-0.4
0.0
Voltage (V)
b
ln(I/V²)
-16.0
-16.3
-16.6
-16.9
-2.0
-1.5
-1.0
-0.5
1/V (V⁻¹)

Figure 5